

# Supplemental material

## REFERENCE

[1] F. Destremes, J. Meunier, M.-F. Giroux, G. Soulez, G. Cloutier, "Segmentation of Plaques in Sequences of Ultrasonic B-Mode Images of Carotid Arteries Based on Motion Estimation and a Bayesian Model", *IEEE Trans. Biomed. Eng.*, 58 (8): 2202-2211, 2011.

## MEAN POINT-TO-POINT AND HAUSDORFF DISTANCES OVER THE DATASET OF ALL IMAGES

We present in Fig. 1 below the histograms of the measures D (mean point-to-point distance) and HD (Hausdorff distance) between the semi-automatic and the manual segmentations over all frames. So, there are images for which the semi-automatic and the manual segmentations do not agree so much, as indicated by the mean values and standard deviations of the eight evaluation measures presented in [1, Tables III and IV].

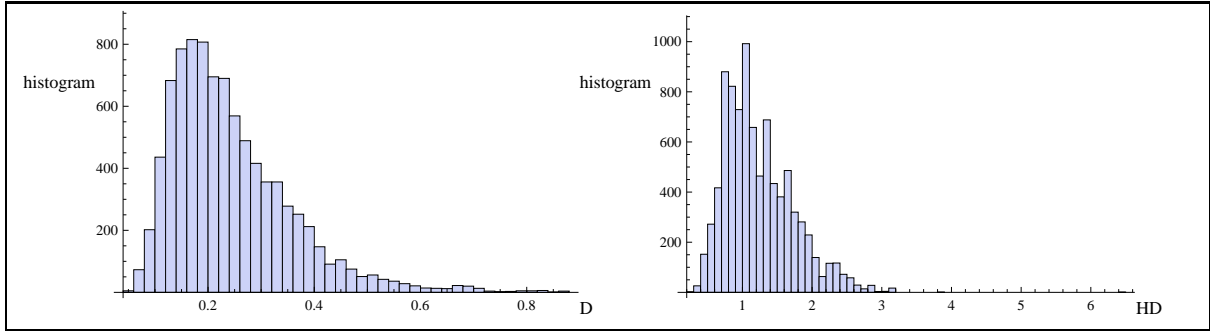


Fig. 1. Histograms of the mean point-to-point distance (D) and of the Hausdorff distance (HD) between the manual and the semi-automatic segmentations over the whole dataset of images.

## THE EIGHT EVALUATION MEASURES OVER THE FRAMES OF ONE EXAMPLE

We present here the eight evaluation measures of the algorithm as a function of the frame number for the video sequence of [1, Fig. 3], first image from the left. As one can see from Fig. 2 and 3 below, there is a variability in the eight measures along cycles in the sequence.

## SUMMARIZE OF THE SEGMENTATION METHOD

### Manual initialization (user dependent)

The plaque in the first frame is segmented manually by an operator, thus yielding two piecewise linear curves  $\gamma_{1,\text{man}}^{(1)}$  and  $\gamma_{2,\text{man}}^{(1)}$ .

### First frame (user independent)

- *Prediction of the position and shape of the plaque.* The manual segmentation serves as prediction for the first frame, i.e. we take  $(\gamma_{1,\text{pred}}^{(1)}, \gamma_{2,\text{pred}}^{(1)}) = (\gamma_{1,\text{man}}^{(1)}, \gamma_{2,\text{man}}^{(1)})$ .
- *Estimation of  $\beta$ .* The parameter  $\beta$  is estimated once and for all for the whole sequence based on the initial manual segmentation  $(\gamma_{1,\text{man}}^{(1)}, \gamma_{2,\text{man}}^{(1)})$  as explained in the Appendix.
- *Region of interest.* Two curves  $\gamma_{-}^{(1)}$  and  $\gamma_{+}^{(1)}$  are obtained by translating  $\gamma_{1,\text{man}}^{(1)}$  2 mm toward the lumen and  $\gamma_{2,\text{man}}^{(1)}$  2 mm toward the adventitia, respectively. This defines a ROI at frame  $t = 1$ .
- *Estimation of the various Nakagami distributions.* The ROI is partitioned into  $B$  non-overlapping vertical strips of about 5 mm wide each. In each vertical strip  $b$ , 800 points between the curves  $\gamma_{-}^{(1)}$  and  $\gamma_{+}^{(1)}$  are chosen randomly according to a uniform distribution. A mixture of three gamma distributions  $\sum_{i=1}^3 p_i \mathcal{G}(I | k_i, \theta_i)$  is

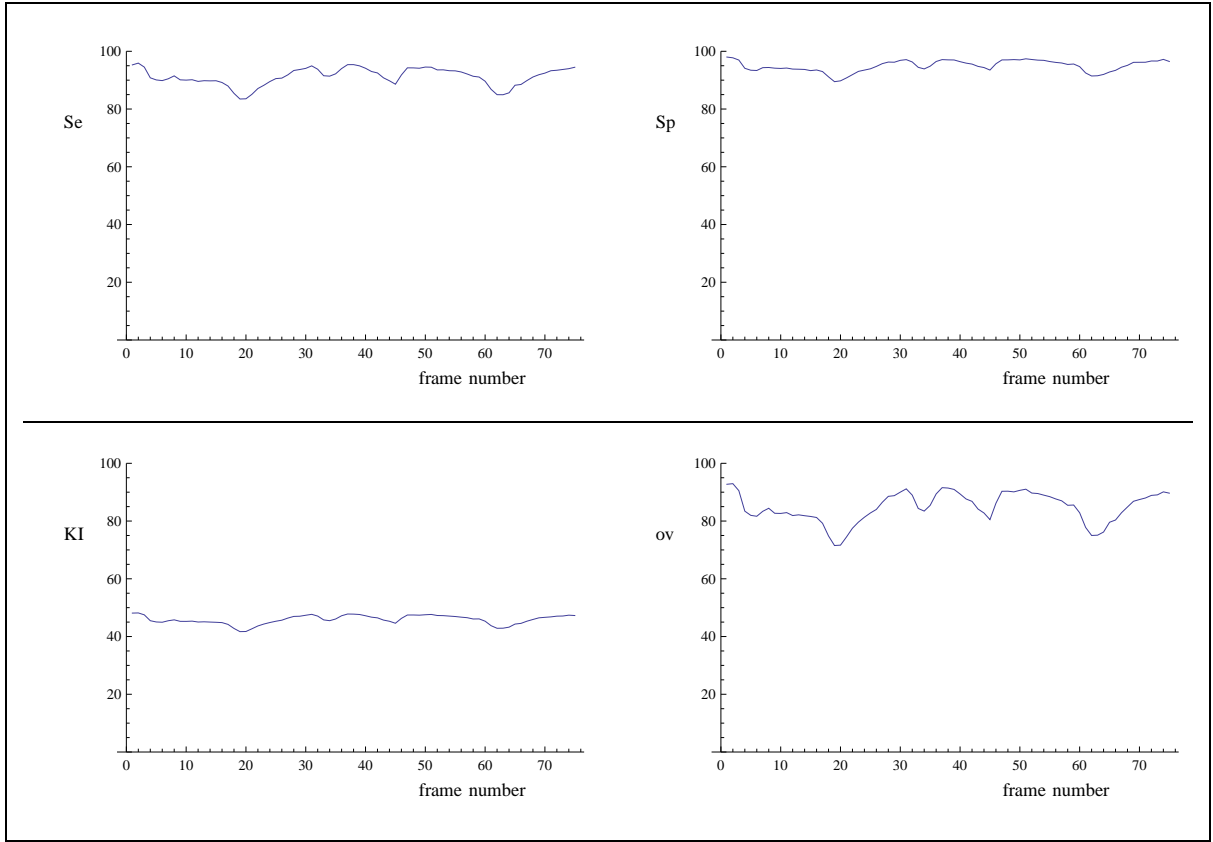


Fig. 2. The evaluation measures se, sp, KI and ov (sensitivity, specificity, kappa index and overlap) as a function of the frame number for the video sequence of [1, Fig. 3], first image from the left. These measures indicate the agreement between the manual and the semi-automatic segmentations (the higher the better).

estimated using the feature  $I^{(1)}$  of the first frame at those 800 points, using the EM algorithm<sup>1</sup> of [15, Table 1]. Here, we drop the indices  $b$  and  $t$ , for simplicity. We use a uniform Dirichlet prior on the proportions  $p_i$ , specified by the hyper-parameters' values  $\alpha_1 = \alpha_2 = \alpha_3 = 1/3$ ,  $A_0 = 3$ , in the model of [15].

- *Estimating the weight of each distribution for each tissue.* For each tissue  $j = 1, 2, 3$  (i.e. lumen, plaque, or adventitia) and each vertical strip  $b$ , the three coefficients  $q_i^j$ ,  $i = 1, 2, 3$ , in Section IV-B, are estimated using the EM algorithm [23].
- *Computation of the likelihood.* The distributions  $f_j^{(1)}$ , for  $j = 1, 2, 3$ , are constructed for each pixel  $s$  in the ROI, as in [15, Eq. (11)].
- *Segmentation.* The continuous piecewise linear curves  $\hat{\gamma}_1^{(1)}$  and  $\hat{\gamma}_2^{(1)}$  located within  $\gamma_-^{(1)}$  and  $\gamma_+^{(1)}$ , that maximize the posterior distribution of Eq. (12) are computed using the stochastic optimization algorithm Exploration/Selection (ES) of [15].

#### Subsequent frames (user independent)

- *Prediction of the position and shape of the plaque.* Given  $t > 1$ , let  $N_t = 21$  (or  $N_t = t$ , if  $t \leq 21$ ), which corresponds to about 1 second of the video-sequence. For each  $t' \in [t - N_t, t - 1]$ , let  $(\tilde{\gamma}_1^{(t')}, \tilde{\gamma}_2^{(t')})$  be the solution at frame  $t'$ . As in Section III-D, we consider the average  $(\gamma_{1,\text{pred}}^{(t)}, \gamma_{2,\text{pred}}^{(t)})$  of the propagations on the time-span  $[t - N_t, t - 1]$ .
- *Region of interest.* Two curves  $\gamma_-^{(t)}$  and  $\gamma_+^{(t)}$  are obtained by translating  $\tilde{\gamma}_1$  2 mm toward the lumen, and  $\tilde{\gamma}_2$  2 mm toward the adventitia, respectively, where  $(\tilde{\gamma}_1, \tilde{\gamma}_2)$  corresponds to the propagation of  $(\gamma_{1,\text{man}}^{(1)}, \gamma_{2,\text{man}}^{(1)})$  from frame 1 to frame  $t$ . This defines a ROI at frame  $t$ . The choice of 2 mm is arbitrary, but it seems amply

<sup>1</sup>In our implementation, a distribution is dropped out whenever its estimated proportion becomes less than 1% (i.e. 8 points out of 800) within the EM algorithm.

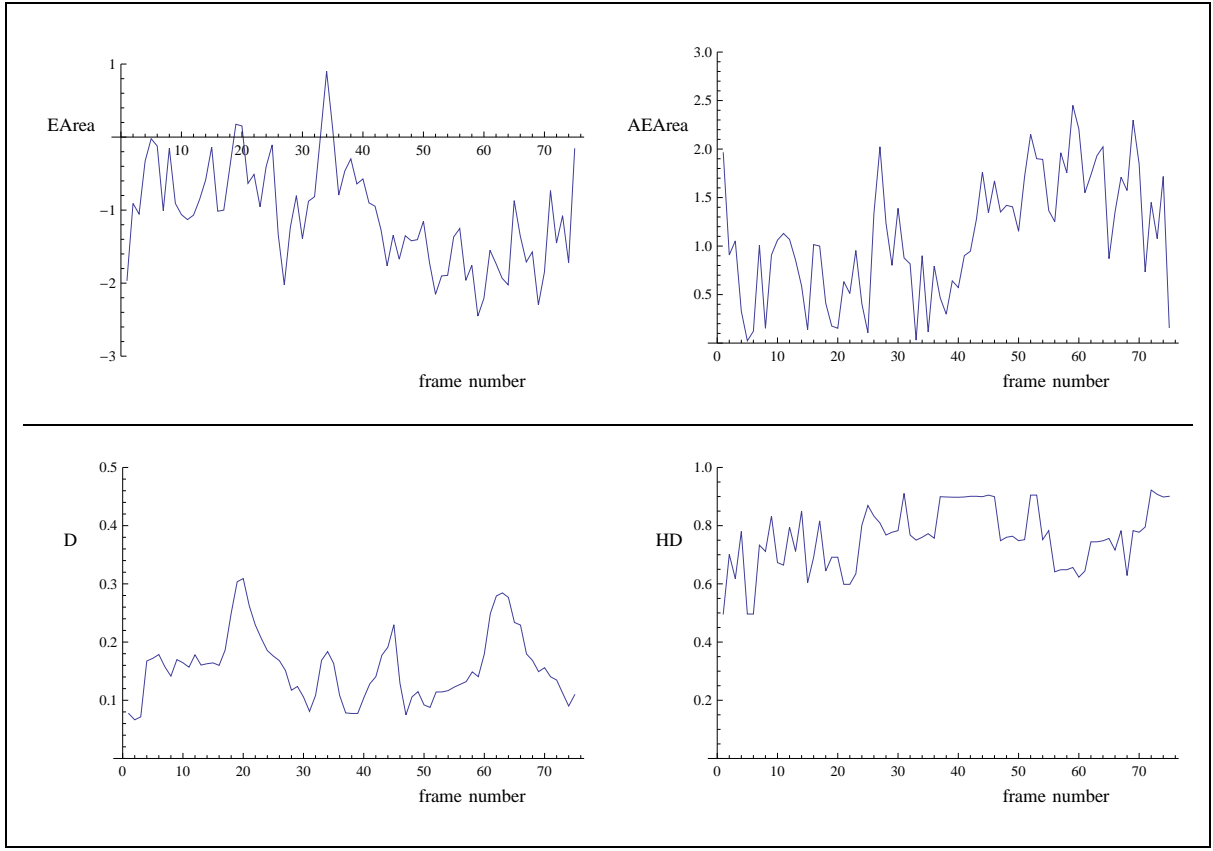


Fig. 3. The evaluation measures EArea, AEArea, D and HD (error of area, absolute error of area, mean point-to-point distance and Hausdorff distance) as a function of the frame number for the video sequence of [1, Fig. 3], first image from the left. The first two measures indicate the agreement between the manual and the semi-automatic segmentations (the higher the better). The other two measures indicate the discrepancy between the manual and the semi-automatic segmentations (the lower the better).

sufficient to allow tracking the movement of the plaque from one frame to the next one due to the dilation of the artery (axial motion) and the propagation of the cardiac pulse pressure (lateral motion), provided the transducer is held fixed.

- *Estimation of the various Nakagami distributions.* In each vertical strip  $b$ , 800 points between the curves  $\gamma_-^{(t)}$  and  $\gamma_+^{(t)}$  are chosen randomly according to a uniform distribution. A mixture of three gamma distributions  $\sum_{i=1}^3 p_i \mathcal{G}(I | k_i, \theta_i)$  is estimated using the feature  $I^{(t)}$  of the first frame at those 800 points, as for the first frame.
- *Estimating the weight of each distribution for each tissue.* The values  $q_i^j$  ( $i, j = 1, 2, 3$ ) are determined from the prediction  $(\gamma_{1,\text{pred}}^{(t)}, \gamma_{2,\text{pred}}^{(t)})$  as for the first frame.
- *Segmentation.* The continuous piecewise linear curves  $\hat{\gamma}_1^{(t)}$  and  $\hat{\gamma}_2^{(t)}$  located within  $\gamma_-^{(t)}$  and  $\gamma_+^{(t)}$ , that maximize the posterior distribution of Eq. (12) are computed using the stochastic optimization algorithm Exploration/Selection (ES) of [15].